Research Article | Vol. 32, No. 12 / 3 Jun 2024 / Optics Express 21149
Optics EXPRESS

Few-cycle pulse retrieval using amplitude swing technique

MIGUEL LÓPEZ-RIPA,[1] ÓSCAR PÉREZ-BENITO,[2] BENJAMÍN ALONSO,[1,3] ROSA WEIGAND,[2] AND ÍÑIGO SOLA[1,3,*]

[1]Grupo de Aplicaciones del Láser y Fotónica (ALF), Departamento de Física Aplicada, Universidad de Salamanca, Plaza de la Merced s/n, 37008 Salamanca, Spain
[2]Department of Optics, Faculty of Physics, University Complutense, Plaza de Ciencias 1, 28040 Madrid, Spain
[3]Unidad de Excelencia en Luz y Materia Estructuradas (LUMES), Universidad de Salamanca, Plaza de la Merced s/n, 37008 Salamanca, Spain
*ijsola@usal.es

Abstract: Ultrashort pulses have garnered significant attention across various scientific disciplines and applications. In this paper, we demonstrate that the recently introduced amplitude swing technique is a robust method for characterizing pulses in the few-cycle temporal domain by analyzing compressed and chirped pulses from a Ti:Sapphire laser oscillator. The duration of the measured pulse for the case of best compression was 5.98 fs (Fourier limit 5.50 fs) corresponding to 2.2 cycles, while the chirped pulses were up to 15 times temporally stretched. The results obtained have been validated using the d-scan technique, showing excellent agreement in all situations. Therefore, the capability of the amplitude swing technique to measure ultra-broadband pulses in the few-cycle regime is demonstrated, as well as very far from optimum compression, while only being limited by the transparency and birefringence of its elements.

1. Introduction

Few-cycle pulses (i.e., those with time duration of the order of a single or just a few optical cycles) have attracted interest the last decades [1] because of their applications to several fields, for example attoscience [2], time-resolved spectroscopy [3] or laser-plasma acceleration [4], to mention some.

The temporal characterization of such short pulses is challenging because of the ultra-broadband spectra involved. Since the beginning of the ultrafast optical technology, several characterization techniques have gained access along the time to this temporal range. The ultrafast optical autocorrelation [5], invented in 1967, FROG [6] and SPIDER [7], introduced in the 90s, are some of the most consolidated ultrashort pulse characterization techniques and they have shown their capabilities to retrieve few-cycle pulses [8–11]. In 2010 the self-referenced spectral interferometry (SRSI) technique [12] was presented and it can be applied to sub-5 fs pulses [13]. Almost at the same time, the dispersion scan (d-scan) technique was developed [14], and it has been shown to be well suited for the measurement in the single- and few-cycle regime [15,16]. Other advanced techniques, such as TIPTOE [17] and attosecond streaking spectrogram [18], can characterize the actual electric field. However, the set-ups required are quite complex.

Recently, a new technique called amplitude swing has been developed [19]. It consists in modulating the relative intensity of two pulse replicas at a given delay, typically of the order of the Fourier Limit (FL) pulse duration. These modulated pulses pass through a nonlinear medium (e.g., a second harmonic generation (SHG) crystal), where the nonlinear signal is generated (SHG signal in this case). Finally, a spectrometer registers the SHG spectrum. While changing the relative amplitude among both replicas, the different SHG spectra are measured, creating a 2D trace. A compact and simple implementation was introduced using a rotating multiple-order

#524427 https://doi.org/10.1364/OE.524427
Journal © 2024 Received 20 Mar 2024; revised 16 May 2024; accepted 17 May 2024; published 23 May 2024

Optics EXPRESS

waveplate (MWP) [19]. Thus, from the projection of a linearly polarized input pulse into the MWP fast and slow axes, two replicas are created, with a certain delay, depending on the thickness and birefringence of the MWP, and a relative amplitude among them depending on the plate orientation angle. The beam passes through a linear polarizer, which selects the polarization projection along its transmission axis. Thus, the resulting modulated replicas enter in a SHG crystal to generate the nonlinear signal, that is analyzed by means of a spectrometer. This simple, in-line and robust set-up, that can be implemented in diverse configurations [20], is made up of common optical materials, and shows a remarkable robustness, being quite resistant to noise and spectral clipping of the signal, including non-ideal SHG response [21]. In addition, since the spectral range of operativity relies on the transparency window of the optical elements and the SHG crystal operation conditions, the same set-up works at very different spectral conditions, being demonstrated within at least more than one octave [22]. The capability of adapting to very broad spectral ranges makes the technique suitable to be adapted to the few-cycle regime, which we will show here. Furthermore, the technique has been shown to retrieve vector pulses (i.e., pulses with time dependent polarization state) [23] without changes in the set-up.

The present work addresses the experimental demonstration of the amplitude swing operativity in the few-cycle regime. This manuscript is structured as follows. Firstly, the material and methods used are commented. Secondly, the results are presented and discussed, validating the operation of the amplitude swing technique at few-cycle regime by comparing it with d-scan measurements. The study includes experiments at situations near and far from pulse compression. Finally, the conclusions are discussed.

2. Materials and methods

In the present work, we study the amplitude swing technique when it is used for characterizing a few-cycle pulse. In particular, the few-cycle laser source is a home-made Ti:Sapphire oscillator [24,25], emitting spectra compatible with FL of 5.50 fs at a repetition rate of 76 MHz and energy per pulse of ~1 nJ.

The validation of amplitude swing as a few-cycle characterization technique is done by comparing its results with a consolidated technique. Here, we choose the d-scan technique because, as previously commented, it is specially well suited for the few-cycle pulse range [14,25,26]. To guarantee that both techniques measure the pulses under the same conditions, we decided to merge both, combining them into a hybrid set-up (Fig. 1). Please note that this combined set-up is made only for comparison purposes.

Firstly, the dispersion is pre-compensated, bouncing three times over each mirror of a pair of chirped mirrors (double CMs or DCMs, model DCM7 from Venteon), which introduces negative dispersion (-120 fs^2 per pair of bounces at λ=800 nm). Therefore, the d-scan can be performed around the phase compensation conditions (i.e., the pulse best compression situation). Then, the laser beam goes through two motorized BK7 glass wedges with an apex angle of 8°, which were used for the d-scan measurement and to control the pulse chirp to be measured with amplitude swing. After that, a rotating 200-μm quartz plate (acting as MWP in the amplitude swing scan) is placed, introducing a 6.58-fs delay between ordinary and extraordinary polarization components at λ=800 nm and with a phase retardation of 0.61π (obviating a 2πm offset) for the same wavelength. After the MWP, a wire grid linear polarizer is placed, set at 0° to select the horizontal projection. Then, the beam is focused using an off-axis parabolic mirror (1-inch focal length) onto a 10-μm Type-I BBO to produce SHG. Finally, the SHG signal is filtered using two colour filters (FGB37 from Thorlabs and BG12 from Schott), removing the remaining fundamental radiation, and it is collected with an UV-Grade Fused Silica lens into an optical fibre connected to a spectrometer (model HR4000 from Ocean Optics Inc.), operating from 196 to 660 nm. Also, the fundamental spectrum can be measured introducing an optical diffuser medium before the BBO crystal and collecting the diffused signal into a spectrometer (USB4000

Optics EXPRESS

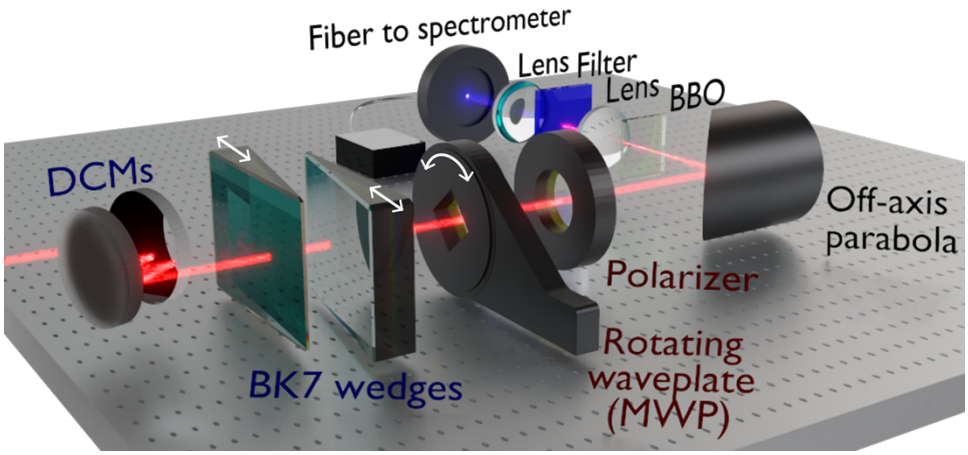

Fig. 1. Experimental set-up. Scheme of the experimental set-up showing simultaneously the d-scan (blue) and the amplitude swing (brown) characterization techniques using the same SHG elements/system (black). During the d-scan measurement the amplitude swing elements are fixed and vice versa.

from Ocean Optics Inc.). Since we use a hybrid set-up to validate the amplitude swing results against the d-scan reconstructions, during the d-scan measurement the SHG spectrum is recorded for different insertions of the motorized wedges, whereas the MWP is fixed with its fast axis at 0°. Alternatively, during the amplitude swing measurement, the wedges are placed at a desired position to study the different cases shown later (pulse compression, negative and positive chirp) and the SHG spectrum is measured for different angles of the MWP.

The amplitude swing retrievals were performed using the Levenberg-Marquardt algorithm [19] to extract the spectral phase of the pulse with two phase optimization steps. The first step optimizes the group delay dispersion (GDD) and third order dispersion (TOD) terms of a Taylor series expansion, and the second step performs a finer adjustment fitting the combination of the GDD, TOD and phase first derivative of the phase at 24 equispaced spectral points (the retrieved values of the phase derivative are interpolated and integrated to yield the retrieved phase that is added to the phase given by the retrieved GDD and TOD values). To compare the retrieved and experimental traces for the optimization, we choose a merit function that compares the absolute difference of the traces. Concerning the d-scan retrievals, the spectral phase is defined as a Fourier series with 15 sine and 15 cosine terms. The retrieved spectral phase is obtained by finding the amplitude of each term using the Quasi Newton Broyden–Fletcher–Goldfarb–Shanno (BFGS) optimization algorithm [25]. The values of those amplitudes are updated iteratively towards obtaining smaller values of the error function (defined as the root mean square error between the measured and the retrieved traces [14]).

Characterizing pulses in the few-cycle regime means dealing with ultra-broadband pulses and their associated problems. For instance, the delay introduced by the MWP varies along the spectrum because of dispersion. As previously commented [19], the delay between the two pulse replicas must be within a certain range around the FL pulse duration (typically between 1/3 and 3 times the FL pulse temporal duration [21]). Despite the spectral dependence of the optical properties of the MWP chosen, the delay is around ~1.1-1.2 times the FL pulse duration and its dispersion is considered in the retrieval algorithm, so it can be used straightforward. Therefore, the delay introduced by amplitude swing can be non-constant, provided that the dispersion of the MWP (and therefore the delay) is known (e.g., from Sellmeier equations and thickness of the material).

Optics EXPRESS

Indeed, one of the main challenges of working with ultra-broadband pulses in this kind of techniques concerns the bandwidth of the nonlinear signal response. In this case the SHG response due to phase matching efficiency, even when using a thin BBO crystal. Due to the large spectral bandwidth of the laser, the SHG response must be properly calibrated for a correct characterization. In the case of d-scan, the SHG response, $R(\omega)$, is directly obtained during the iterative retrieval algorithm by comparison of the experimental and simulated traces using the following equation [14]:

$$R_{\mathrm{Dscan}}(\omega) = \frac{\sum_k I_{\mathrm{meas}}(\omega, z_k) \cdot I_{\mathrm{sim}}(\omega, z_k)}{\sum_k I^2_{\mathrm{sim}}(\omega, z_k)} \tag{1}$$

where, I_{meas} and I_{sim} are the experimentally measured and simulated d-scan traces respectively, which depend on z_k, the thickness of the glass at a certain insertion position k of the pair of wedges, and the angular frequency ω. Please notice that the SHG response above mentioned is sometimes defined in the literature as $\mu_{\mathrm{Dscan}}(\omega)$.

Regarding amplitude swing, the SHG response can also be obtained in the retrieval algorithm [21]. However, we have observed that this approach, while working properly near FL pulse conditions, can be troublesome in terms of retrieval convergence for highly chirped pulses with ultra-broadband spectra, such as the most chirped situations that are studied in this work. This situation appears because the frequency marginals of the SHG traces present important null signal areas and, in addition, they show a coupling between the unknown spectral phase and the SHG response function, also unknown [21]. To solve this issue, we decided to model the theoretical SHG response of the system and consider it in the amplitude swing algorithm.

The theoretical SHG response of the system can be obtained from the combination of the frequency-dependent transmission and sensitivity of the detection systems and the spectral response of the nonlinear medium for the SHG process [8]. On one hand, the response of the detection system can be expressed as the combination of the colour and neutral filters used to select the SHG signal (R_{Filters}) and the spectrometer (R_{HR4000}) responses (depicted as orange and yellow curves of Fig. 2(a)). In this case, the filters response was given by the manufacturer, and the fibre spectrometer response was experimentally calibrated measuring the emission spectrum of a calibration white lamp with an integrating sphere (AvaLight-HAL-CAL ISP30 from Avantes). On the other hand, the theoretical response of the nonlinear medium (green curve of Fig. 2(a)) includes the phase-matching efficiency dependence ('sinc' term) weighted with the second order susceptibility of the refractive index ($\chi^{(2)}$). Therefore, the theoretical SHG response of the system, will be given by [8]:

$$R_{\mathrm{Theo}}(2\omega) = \frac{(2\omega)^3}{n_{\mathrm{e}}(2\omega)} \cdot R_{\mathrm{Filters}}(2\omega) \cdot R_{\mathrm{HR4000}}(2\omega) \cdot |\chi^{(2)}(2\omega)|^2 \cdot \mathrm{sinc}^2\left[\frac{\Delta k(2\omega) L}{2}\right] \tag{2}$$

where $\chi^{(2)}(2\omega) = [(n_{\mathrm{e}}(2\omega))^2 - 1][(n_{\mathrm{o}}(\omega))^2 - 1]^2$ and $\Delta k(2\omega) = \frac{2\omega}{c}(n_{\mathrm{e}}(2\omega) - n_{\mathrm{o}}(\omega))$ is the phase-mismatch, being n_{o} and n_{e} the ordinary and extraordinary refractive indices of the type-I BBO, which can be calculated using Sellmeier equations [27] and knowing the crystal cut angle (29.2°), and its thickness L (10 µm in our case). The resulting theoretical SHG response is compared with the one obtained using the d-scan technique in Fig. 2(b), showing good agreement but with some differences. Firstly, the d-scan SHG response is represented for a shorter spectral range corresponding to the regions with non-zero signal where the d-scan retrieval is optimized. Secondly, the d-scan SHG response is slightly lower around λ=425 nm, while this is not observed in the theoretical response. A possible explanation for this difference may be a small and non-significant artifact of the d-scan retrieval because this area matches with the lowest SHG (and the corresponding fundamental) signal region or a slight deviation in the theoretical calibration. Anyway, we have observed that the retrieval tolerates this kind of deviation in the SHG response

Optics EXPRESS

calibration in the cases under study, as it is demonstrated in the Supplemental Material (see Supplement 1), where we compare the amplitude swing retrievals considering the theoretical SHG response and the one obtained from the d-scan, finding that in both cases the retrieved pulse is the same.

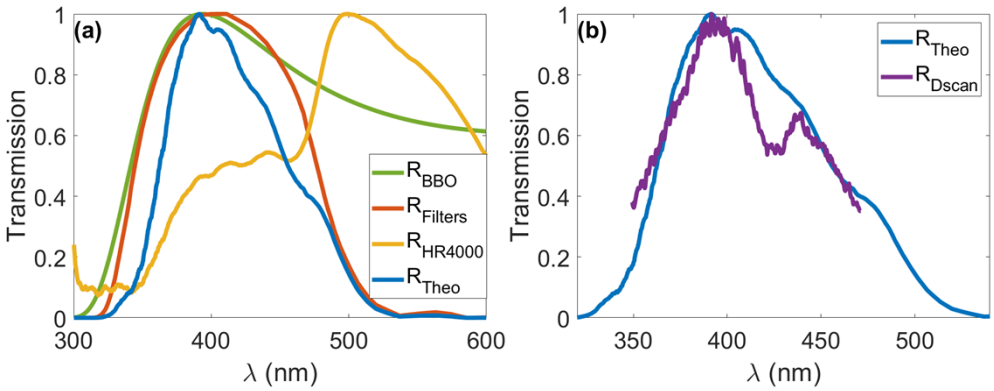

Fig. 2. SHG response. (a) Theoretical simulation of the system SHG response (blue), obtained from the combination of the BBO theoretical response (green) and the spectral dependence of the filters used to select the signal (orange) and spectrometer (yellow). (b) Comparison of the theoretical SHG response (blue) and the one experimentally obtained in the d-scan retrieval (purple).

Please note that the nonlinear crystal theoretical response related to the phase matching efficiency is derived for a monochromatic case. To assess its validity for an ultrabroadband pulse, we calculated the SHG field of the pulse from its autoconvolution in the spectral domain. This way, the phase mismatch can be computed for the sum of frequencies of all possible pairs of fundamental frequencies leading to a given SHG frequency, then calculating its integrated effect. We tested different pulses (near and far from compression, with different spectral amplitudes) and different nonlinear crystals (thickness and central phase matching wavelength), always finding that the integrated effect can be modeled as the response for a continuous wave without any deviation.

In the amplitude swing retrievals, as previously commented, we used the theoretical SHG response and optimized the retrieved trace in the spectral range with significant signal (λ= 348-468 nm), avoiding areas with low signal. By doing so, the amplitude swing reconstructions are self-consistent and do not depend on the response obtained from another external measurement (e.g., the one obtained from the d-scan, which is used here just to validate the amplitude swing results). Indeed, it is easy to estimate it, as it is done here, since the phase-matching curve of a BBO crystal is well known and the spectral response of the filters is usually given by the manufacturer. Nevertheless, other strategies could be used to obtain the SHG response. For example, it can be experimentally calibrated using a known reference pulse with equal or broader bandwidth.

3. Results and discussion

The versatility of amplitude swing enables to characterize pulses in different spectral regions [22]. In addition, provided that the MWP delay is comparable to the FL temporal duration, amplitude swing can characterize highly chirped pulses. Taking this into account, firstly the beam will be characterized for the insertion of the wedges at the maximum compression point (i.e., the position that compensate chirp better), and then for other insertion positions of the wedges to have negative and positive chirp values.

Optics EXPRESS

In a first set of experiments, the pulse was measured at the maximum compression point. As shown later in the results (Fig. 3), at this position the pulse is not a FL pulse due to the residual phase that cannot be perfectly compensated by the dispersion of the wedges and the DCMs, but it is quite close to FL anyway. Figure 3 shows the characterization obtained with both techniques. The amplitude swing measurement was performed at the maximum compression position of the wedges that remained fixed, as mentioned before. Notice that to measure the pulse, the d-scan requires scanning the pulse dispersion around compression by controlling the wedge insertion (i.e., the effective thickness of the wedges pair). Firstly, Figs. 3(a1,a2) show the experimental and retrieved amplitude swing traces. Secondly, Figs. 3(b1,b2) correspond to the experimental and retrieved d-scan traces (notice that the response R_{Dscan} of Fig. 2(b) has been obtained from this retrieval, Eq. (1)). The glass insertion axis corresponding to the wedges adjustable thickness is shown referred to the maximum compression position (0 mm). Therefore, positive (negative) insertion of material corresponds to positively (negatively) chirped pulses. Finally, Figs. 3(c1,c2) show the spectral and temporal comparison of both retrievals for the wedge insertion corresponding to the maximum compression point.

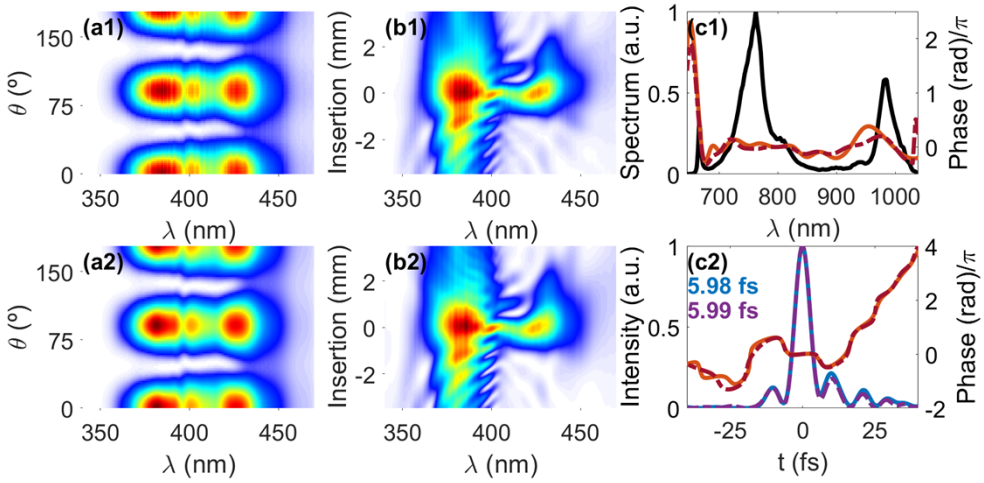

Fig. 3. Near FL pulse characterization. (a1) Experimental and (a2) retrieved amplitude swing traces, (b1) experimental and (b2) retrieved d-scan traces. Comparison of the electric field retrieved at insertion 0 mm in: (c1) spectral domain (black line: the measured spectral intensity; solid orange line: amplitude swing retrieved spectral phase; dashed red line: d-scan retrieved spectral phase) and (c2) temporal domain (solid orange line: amplitude swing retrieved temporal phase; solid blue line: amplitude swing retrieved pulse intensity; dashed red line: d-scan retrieved temporal phase; dashed purple line: d-scan retrieved pulse intensity). An inset of the temporal intensity FWHM of amplitude swing (blue) and d-scan (purple) is included in (c2).

There is a very good agreement between both retrievals, which is also supported presenting very similar pulse duration at Full Width at Half Maximum (FWHM), 5.98 fs and 5.99 fs for the amplitude swing and d-scan, respectively. Regarding the temporal duration of a single cycle for the carrier wavelength of the spectrum, calculated as the gravity centre of the spectrum (2.70 fs at λ=810 nm), the retrieved pulse corresponds to a 2.2-cycles pulse (FWHM). Furthermore, these values are close to the FL temporal FWHM, which in this case is 5.50 fs.

In addition to characterizing the pulse at the compensated dispersion position of the wedges, the versatility of amplitude swing enables to measure the pulse with different dispersion values, which is interesting in situations where the pulse does not need to be compressed in any moment.

Optics EXPRESS

To demonstrate this, the pulse was characterized also for different insertion of the wedges out of compression. For the validation of the amplitude swing results in these situations we compared with the pulse obtained with the d-scan for the corresponding glass insertion.

In Fig. 4 the experimental (first and third rows) and retrieved (second and fourth rows) amplitude swing traces are shown, obtained introducing a controlled dispersion by setting the wedges at given positions with respect to the maximum compression point. The measured positions corresponded to 8 wedge insertions in steps of 0.878 mm (both for negative and positive chirp) up to ±3.512 mm. Provided that the group delay dispersion of BK7 is 43.71 fs^2/mm at 810 nm, at each step we add to the pulse a GDD of 38.4 fs^2, while reaching a total GDD of ±153.6 fs^2 at the extreme cases with respect to compression. The results shown in Fig. 4(a-h) are ordered from negative to positive wedge insertion and dispersion. Please note that the phase added is the actual phase of BK7, not a pure GDD, but we provide here the GDD value to illustrate the amount of pulse dispersion.

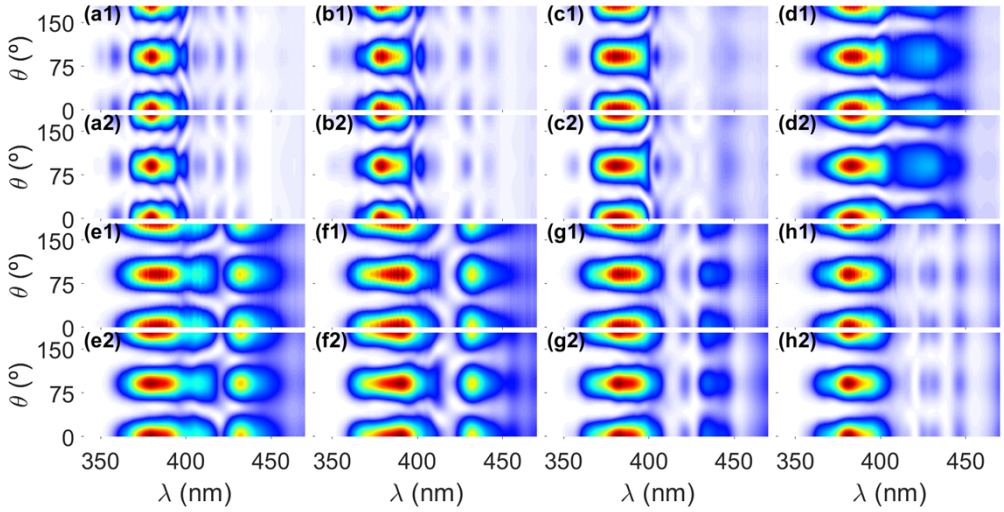

Fig. 4. Amplitude swing traces for pulses far from FL conditions. Experimental (first and third rows) and retrieved (second and fourth rows) amplitude swing traces for different insertions of the wedges corresponding to a relative added dispersion respect to the compensated position of (a) –3.512 mm (–153.6 fs^2), (b) –2.634 mm (–115.2 fs^2), (c) –1.756 mm (–76.8 fs^2), (d) –0.878 mm (–38.4 fs^2), (e) + 0.878 mm (+38.4 fs^2), (f) + 1.756 mm (+76.8 fs^2), (g) + 2.634 mm (+115.2 fs^2) and (h) + 3.512 mm (+153.6 fs^2).

The corresponding pulse and phase retrievals are shown in Fig. 5. On one hand, Figs. 5 (a1-h1) depict the spectral phase comparison between the amplitude swing and d-scan retrievals for each added dispersion value. On the other hand, the temporal electric field comparison is shown in Figs. 5 (a2-h2). Moreover, an inset of the pulse duration (FWHM) from amplitude swing (blue) and d-scan (purple) is shown for each temporal retrieval. The comparison in both, the spectral and temporal domains, present excellent agreement for each dispersion value, even far from maximum compression point. Notice that the pulse is stretched up to ~15-20 times its FL pulse duration, highlighting that the amplitude swing technique is operative under a wide range of chirp.

Optics EXPRESS

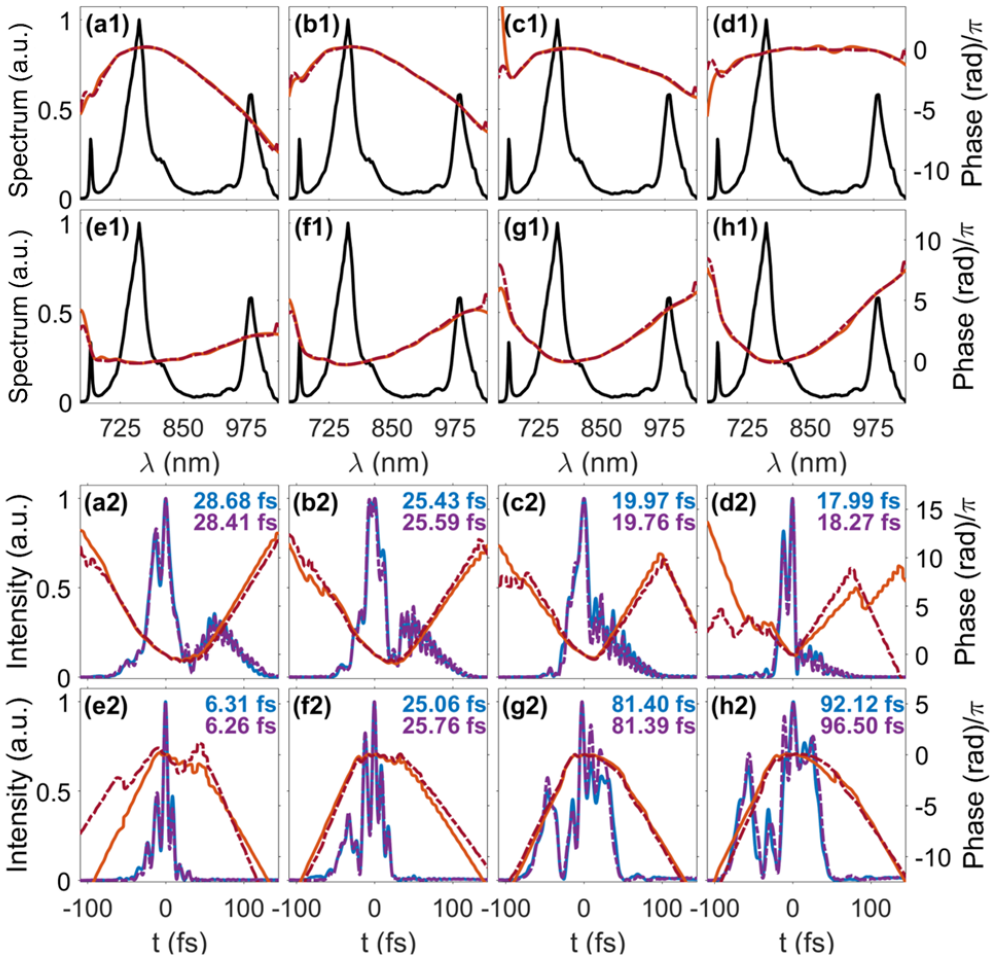

Fig. 5. Comparison among amplitude swing and d-scan retrievals for pulses far from FL conditions. Comparison in the spectral (first and second rows) and temporal (third and fourth rows) domains obtained with amplitude swing (solid lines: orange, phase; blue, pulse time intensity) and d-scan (dashed lines: red, phase; purple, pulse time intensity) for the relative added dispersion values of (a) –3.512 mm (–153.6 fs^2), (b) –2.634 mm (–115.2 fs^2), (c) –1.756 mm (–76.8 fs^2), (d) –0.878 mm (–38.4 fs^2), (e) +0.878 mm (+38.4 fs^2), (f) +1.756 mm (+76.8 fs^2), (g) +2.634 mm (+115.2 fs^2) and (h) +3.512 mm (+153.6 fs^2). The black line stands for the measured spectral intensity. An inset of the temporal intensity FWHM of amplitude swing (blue) and d-scan (purple) is included in e2-h2.

Optics EXPRESS

4. Conclusions

In the present work the performance of the amplitude swing technique in the few-cycle pulse regime has been demonstrated. For this purpose, it has been compared and validated with the d-scan technique. The results obtained with amplitude swing present an excellent match with the validating measurements, both for near and far from FL pulse conditions.

The study has also highlighted the importance of knowing the proper SHG response function. Some options consist of calibrating the response of the SHG system from the amplitude swing measurement itself [21], using the function obtained from other technique (e.g., d-scan) or calculating the theoretical response [8]. Here, we have used the latter, obtaining a very good match. Therefore, the use of the theoretical response has been validated and constitutes a very convenient alternative to the extraction of the SHG response directly from the amplitude swing trace.

In addition, the versatility of the amplitude swing technique enables the possibility to characterize the ultra-broadband pulses without needing to compress them, allowing both near- and far-FL pulse conditions, as shown with the chirped pulse reconstructions very far from compression.

Thus, the amplitude swing technique can characterize few-cycle laser pulses, a very delicate and complex regime, without significantly modifying the original scheme [19], which is quite simple, robust, and compact, including elements commonly found at a laser laboratory (e.g., linear polarizers, MWP, BBO crystals). The only considerations that need to be done are to use a MWP introducing a delay of the order of the FL pulse duration and a good calibration (either experimental or theoretical) of the SHG response. Therefore, a full flat SHG phase matching condition is not mandatory [21].

As recently demonstrated [22], amplitude swing can operate along a broad spectral range, more than one octave (from 620 nm to 1550 nm central wavelength, but with the potential of being broader) without significant changes in the set-up, only limited by the transparency window of the components and the requirements of the nonlinear signal emission (e.g., the SHG phase matching) and detection. Therefore, the technique has the potential of characterizing even shorter pulses (i.e., presenting broader spectra) and it is not restricted to the Ti:Sapphire emission band (e.g., further in the IR and mid IR region), increasing its range of applicability while maintaining its simplicity and stability.

5. Appendix A: description of the methods

5.1 Models for the characterization techniques

The amplitude swing technique encodes the spectral phase of a pulse under test in a two-dimensional SHG trace [19]. If the electric field is defined as $E(\omega) = A(\omega)e^{i\varphi(\omega)}$, where $A(\omega)$ is the spectral amplitude calculated from the measured power spectrum ($S(\omega)$), being $A(\omega) = \sqrt{S(\omega)}$, and $\varphi(\omega)$ is the spectral phase, the SHG amplitude swing trace ($S^{\mathrm{SHG}}(\omega, \theta)$) is given by:

$$S^{\mathrm{SHG}}(\omega,\theta) = \left| \int \left(\int A(\omega') e^{i\varphi(\omega)} [e^{i\rho_{\mathrm{f}}(\omega')} \cos^2\theta + e^{i\rho_{\mathrm{s}}(\omega')} \sin^2\theta] e^{i\omega' t} d\omega' \right)^2 e^{-i\omega t} dt \right|^2 \tag{3}$$

being ω and θ the spectral frequency and the angle between the fast axis of the MWP and the horizontal direction, respectively. In addition, $\rho_{\mathrm{f}}(\omega)$ and $\rho_{\mathrm{s}}(\omega)$ correspond to the phase terms acquired due to travel through the fast and slow axes of the MWP. Note that the SHG signal in Eq. (3) is given for an ideal trace with perfect phase matching and flat spectral response of the detection system. In the present case of few-cycle pulses, due to their ultrabroadband nature, the calculated ideal trace must be multiplied by the spectral response given in Eq. (2) before comparing it to the experimental trace in the reconstruction algorithm.

Optics EXPRESS

5.2 Calibrations

Before doing the amplitude swing retrievals, it is necessary to properly calibrate the MWP or to use the manufacturer nominal values. In particular, it is required to know the relative phase between the fast and slow axes. As done in previous works [19–23], here the phase retardation (zeroth-order phase) of the MWP was carefully calibrated using inline single-channel spectral interferometry [28] and the spectral dependence was obtained using Sellmeier equations for quartz [29] and knowing the MWP thickness.

Funding. Universidad Complutense de Madrid (CT63/19-CT64/19); Ministerio de Economía y Competitividad (EQC2018-004117-P); Ministerio de Ciencia e Innovación (PID2020-119818GB-I00, PID2022-136260NB-I00); European Regional Development Fund (SA136P20); Consejería de Educación, Junta de Castilla y León (SA136P20).

Disclosures. IS: Universidad de Salamanca (P), BA: Universidad de Salamanca (P).

Data availability. Data underlying the results presented in this paper are not publicly available at this time but may be obtained from the authors upon reasonable request.

Supplemental document. See Supplement 1 for supporting content.

References

1. T. Brabec and F. Krausz, "Intense few-cycle laser fields: Frontiers of nonlinear optics," Rev. Mod. Phys. **72**(2), 545–591 (2000).
2. F. J. Furch, T. Witting, M. Osolodkov, *et al.*, "High power, high repetition rate laser-based sources for attosecond science," J. Phys. Photonics **4**(3), 032001 (2022).
3. H. Kuramochi, S. Takeuchi, and T. Tahara, "Femtosecond time-resolved impulsive stimulated Raman spectroscopy using sub-7-fs pulses: Apparatus and applications," Rev. Sci. Instrum. **87**(4), 043107 (2016).
4. J. Faure, D. Gustas, D. Guénot, *et al.*, "A review of recent progress on laser-plasma acceleration at kHz repetition rate," Plasma Phys. Control. Fusion **61**(1), 014012 (2019).
5. J. A. Armstrong, "Measurement of picosecond laser pulse widths," Appl. Phys. Lett. **10**(1), 16–18 (1967).
6. D. J. Kane and R. Trebino, "Characterization of arbitrary femtosecond pulses using frequency-resolved optical gating," IEEE J. Quantum Electron. **29**(2), 571–579 (1993).
7. C. Iaconis and I. A. Walmsley, "Spectral phase interferometry for direct electric-field reconstruction of ultrashort optical pulses," Opt. Lett. **23**(10), 792–794 (1998).
8. A. Baltuska, M. S. Pshenichnikov, and D. A. Wiersma, "Second-harmonic generation frequency-resolved optical gating in the single-cycle regime," IEEE J. Quantum Electron. **35**(4), 459–478 (1999).
9. G. Steinmeyer, D. H. Sutter, L. Gallmann, *et al.*, "Frontiers in ultrashort pulse generation: pushing the limits in linear and nonlinear optics," Science **286**(5444), 1507–1512 (1999).
10. L. Gallmann, D. H. Sutter, N. Matuschek, *et al.*, "Characterization of sub-6-fs optical pulses with spectral phase interferometry for direct electric-field reconstruction," Opt. Lett. **24**(18), 1314–1316 (1999).
11. M. T. Asaki, C.-P. Huang, D. Garvey, *et al.*, "Generation of 11-fs pulses from a self-mode-locked Ti:sapphire laser," Opt. Lett. **18**(12), 977–979 (1993).
12. T. Oksenhendler, S. Coudreau, N. Forget, *et al.*, "Self-referenced spectral interferometry," Appl. Phys. B **99**(1-2), 7–12 (2010).
13. A. Trabattoni, T. Oksenhendler, H. Jousselin, *et al.*, "Self-referenced spectral interferometry for single-shot measurement of sub-5-fs pulses," Rev. Sci. Instrum. **86**(11), 113106 (2015).
14. M. Miranda, C. L. Arnold, T. Fordell, *et al.*, "Characterization of broadband few-cycle laser pulses with the d-scan technique," Opt. Express **20**(17), 18732–18743 (2012).
15. F. Silva, B. Alonso, W. Holgado, *et al.*, "Strategies for achieving intense single-cycle pulses with in-line post-compression setups," Opt. Lett. **43**(2), 337–340 (2018).
16. H. Timmers, Y. Kobayashi, K. F. Chang, *et al.*, "Generating high-contrast, near single-cycle waveforms with third-order dispersion compensation," Opt. Lett. **42**(4), 811–814 (2017).
17. S. B. Park, K. Kim, W. Cho, *et al.*, "Direct sampling of a light wave in air," Optica **5**(4), 402–408 (2018).
18. A. Wirth, M. Th. Hassan, I Grguraš, *et al.*, "Synthesized Light Transients," Science **334**(6053), 195 (2011).
19. B. Alonso, W. Holgado, and I. J. Sola, "Compact in-line temporal measurement of laser pulses with amplitude swing," Opt. Express **28**(10), 15625–15640 (2020).
20. M. López-Ripa, Í. J. Sola, and B. Alonso, "Generalizing amplitude swing modulation for versatile ultrashort pulse measurement," Opt. Express **31**(21), 34428–34442 (2023).
21. I. J. Sola and B. Alonso, "Robustness and capabilities of ultrashort laser pulses characterization with amplitude swing," Sci. Rep. **10**(1), 18364 (2020).
22. M. López-Ripa, Í. J. Sola, and B. Alonso, "Amplitude swing ultrashort pulse characterization across visible to near-infrared," Opt. Laser Technol. **164**, 109492 (2023).
23. C. Barbero, B. Alonso, and Í. J. Sola, "Characterization of ultrashort vector pulses from a single amplitude swing measurement," Opt. Express **32**(7), 10862–10873 (2024).

Optics EXPRESS

24. R. Weigand, M. Miranda, and H. Crespo, "Oscilador láser de titanio: zafiro de 2 ciclos ópticos," Opt. Pura Apl. **46**(2), 105–110 (2013).
25. O. Pérez-Benito and R. Weigand, "Nano dispersion scan: measurement of sub-7-fs laser pulses using second-harmonic nanoparticles," Opt. Lett. **44**(20), 4921–4924 (2019).
26. F. J. Salgado-Remacha, B. Alonso, H. Crespo, *et al.*, "Single-shot d-scan technique for ultrashort laser pulse characterization using transverse second-harmonic generation in random nonlinear crystals," Opt. Lett. **45**(14), 3925–3928 (2020).
27. G. Tamošauskas, G. Beresnevičius, D. Gadonas, *et al.*, "Transmittance and phase matching of BBO crystal in the 3-5 µm range and its application for the characterization of mid-infrared laser pulses," Opt. Mater. Express **8**(6), 1410–1418 (2018).
28. B. Alonso and I. Sola, "Measurement of Ultrashort Vector Pulses from Polarization Gates by In-Line, Single-Channel Spectral Interferometry," IEEE J. Select. Topics Quantum Electron. **25**(4), 1–7 (2019).
29. G. Ghosh, "Dispersion-equation coefficients for the refractive index and birefringence of calcite and quartz crystals," Opt. Commun. **163**(1-3), 95–102 (1999).